RAPID COMMUNICATION | APRIL 15 2026

Translational and rotational temperature difference in coexisting phases of inertial active dumbbells FREE

Special Collection: Festschrift in honor of Kurt Kremer: Computational Polymer Science and Soft Matter Physics

Subhasish Chaki ; Hartmut Löwen

J. Chem. Phys. 164, 151101 (2026)
https://doi.org/10.1063/5.0324875

The Journal of Chemical Physics COMMUNICATION pubs.aip.org/aip/jcp

Translational and rotational temperature difference in coexisting phases of inertial active dumbbells

Cite as: J. Chem. Phys. 164, 151101 (2026); doi: 10.1063/5.0324875
Submitted: 27 January 2026 • Accepted: 30 March 2026 •
Published Online: 15 April 2026

Subhasish Chaki[a] and Hartmut Löwen

AFFILIATIONS

Institut für Theoretische Physik II: Weiche Materie, Heinrich-Heine-Universität Düsseldorf, Universitätsstraße 1, D-40225 Düsseldorf, Germany

Note: This paper is part of the JCP Festschrift in Honor of Kurt Kremer.
[a]**Author to whom correspondence should be addressed:** subhasischaki@gmail.com

ABSTRACT

We investigate the effect of translational and rotational inertia on motility-induced phase separation in underdamped active dumbbells and identify the emergence of four distinct kinetic temperatures across the coexisting phases—unlike in overdamped systems. We find that the dilute, gas-like phase consistently exhibits a higher translational kinetic temperature than the dense, liquid-like phase, with this difference amplified by increasing the rotational inertia. Rotational kinetic temperatures display a similar trend, with the dense phase remaining colder than the dilute phase; however, in this case, the temperature difference grows with translational inertia and activity while becoming practically independent of rotational inertia. This counterintuitive behavior arises from the interplay of activity-driven collisions with both translational and rotational inertia in the coexisting phases. Our results highlight the critical role of translational and rotational inertia in shaping the kinetic temperature landscape of motility-induced phase separation and offer new insights into the nonequilibrium thermodynamics of active matter.

I. INTRODUCTION

Active particles continuously consume energy from their surroundings at the individual level and convert it into directed or persistent motion.[1–7] As a result, their dynamics fundamentally deviate from those of passive Brownian particles, exhibiting non-equilibrium behavior across a wide range of length scales. Prominent examples include synthetic active colloids,[8,9] motile bacteria,[10,11] crawling cells,[12,13] and even larger-scale organisms such as fish, birds,[14] and insects. A key signature of this non-equilibrium nature is the violation of the fluctuation–dissipation theorem, which manifests in the enhanced long-time diffusion due to persistent motion. Importantly, this persistence not only governs single-particle dynamics but also plays a central role in collective phenomena such as motility-induced phase separation (MIPS),[8,15–20] where, beyond a threshold in activity and density, the system spontaneously separates into a dense phase and a dilute phase in the absence of attractive interactions or alignment.

At the microscale, particle inertia is negligible compared to viscous drag from the surrounding solvent. As a result, the instantaneous velocity of an individual particle (distinct from the coarse-grained velocity arising from self-propulsion) relaxes rapidly, leading to overdamped dynamics. In such systems, MIPS closely resembles equilibrium liquid–gas coexistence, with equal kinetic temperatures in both phases. In contrast, for macroscopic active particles where inertia cannot be neglected,[21] the behavior of MIPS is qualitatively altered. In the dense phase, inertial particles repeatedly bounce back upon collisions, a mechanism that generates a hotter gas-like phase compared to the liquid-like phase and can significantly suppress phase separation.[22–24] Such unequal temperatures between coexisting phases do not necessarily imply the presence of an effective heat flux in the thermodynamic sense driving the system toward equilibrium. Instead, the steady state is maintained by continuous energy input away from equilibrium, which compensates for the dissipation and sustains the temperature difference. Interestingly, Caprini *et al.* demonstrated that rotational inertia, unlike translational inertia, favors MIPS by enhancing the effective persistence time of particle trajectories.[25] In another study, MIPS has been observed in systems of soft self-propelled disks in the overdamped limit, whereas inertial disks exhibit MIPS only in the hard

particle limit.[24,26] More recently, Hecht *et al.* investigated the mixtures of overdamped active and inertial passive Brownian particles,[27] finding that the dense, liquid-like phase can be either colder or hotter than the surrounding dilute, gas-like phase—highlighting the complex interplay between collective behavior and inertia. The temperature difference across coexisting phases in MIPS depends on the definition of temperature. Different definitions of temperature—all coinciding in equilibrium—generally differ in active systems.[28] In overdamped active particles, the notion of kinetic temperature derived from mean-square velocity fluctuations is not meaningful, since velocities are not independent dynamical variables but fully determined by the instantaneous forces. Consequently, no difference in kinetic temperature between coexisting phases arises in the overdamped limit. However, alternative effective temperatures, such as those defined via long-time mean-squared displacement, can differ between coexisting phases of overdamped MIPS due to the reduced particle mobility in dense regions. A difference in kinetic temperature between coexisting phases arises only in the underdamped regime, where inertia gives a meaningful definition of velocity fluctuations. In that regime, collisional effects in dense regions can reduce kinetic fluctuations, leading to distinct kinetic temperatures across phases.

While most studies on motility-induced phase separation (MIPS) focus on active particles with spherical shapes, natural and artificial active matter systems are predominantly composed of anisotropic particles. Notable examples of anisotropic active matter include rod-shaped bacteria,[29] chemically powered nanorods,[30] and vibrated granular rods.[31] Unlike active disks, active rods can slide past one another and, thus, typically do not exhibit MIPS.[32,33] However, Suma *et al.* investigated the phase behavior of a suspension of overdamped active rigid dumbbells and demonstrated that the region of phase space where phase separation occurs is significantly broader than that observed for overdamped spherical active particles.[34–36]

The impact of inertia on the shape and dynamics of macroscopic active systems remains an open and largely unexplored question. To investigate the role of inertia in anisotropic systems, we study a collection of active rigid dumbbells where the active force is applied along their main axis. We focus on uncovering a related and previously overlooked phenomenon: the emergence of a kinetic temperature gradient between coexisting phases in inertial anisotropic active matter. In particular, we examine how inertia influences the rotational kinetic temperature in these phases—a feature absent in spherical particles, where rotational dynamics are decoupled from activity.[37–40] We reveal a mechanism by which rotational inertia gives rise to a kinetic temperature difference between coexisting phases. These findings offer new insights and potential strategies for controlling temperature gradients in the rapidly growing field of macroscopic active matter.[28,41,42]

This paper is structured as follows: After introducing the model in Sec. II, we numerically study the translational and rotational temperature difference in dense and dilute phases of inertial active dumbbells in Sec. III. Finally, we present the conclusion in Sec. IV.

II. MODEL

We consider a two-dimensional system of N self-propelled rigid dumbbells confined in a square box of side length L with periodic boundary conditions. Figure 1 represents an illustration of the system. Each rigid dumbbell consists of two spherical beads of diameter σ_d and mass m, and the center-to-center distance between the beads is fixed at σ_d. The position $\mathbf{r}_i^{(j)}(t)$ of the jth bead of the ith dumbbell evolves in time according to the underdamped Langevin equation,

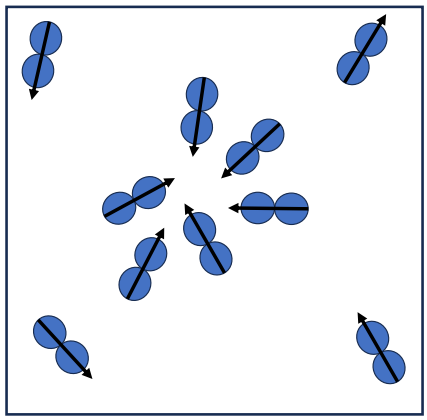

FIG. 1. Schematic illustration of active dumbbells. Induced by a spontaneous fluctuation, a subset of dumbbells moves toward a common center, leading to the formation of a cluster. Arrows indicate the instantaneous self-propulsion directions.

$$m\ddot{\boldsymbol{r}}_i^{(j)} = -\gamma \dot{\boldsymbol{r}}_i^{(j)} + \nabla_i^{(j)} U + \boldsymbol{\xi}_i^{(j)} + \boldsymbol{F}_i^{\mathrm{act}}, \tag{1}$$

where $i = 1, \ldots, N$, $j = 1, 2$, γ is the viscous damping coefficient, U denotes the total interaction potential energy, and $\mathbf{F}_i^{\mathrm{act}}$ represents the self-propulsion force. Beads belonging to different dumbbells interact via a generalized Mie potential, defined as $U(r) = \left\{4\epsilon\left[\left(\frac{\sigma}{r}\right)^{2n} - \left(\frac{\sigma}{r}\right)^{n}\right] + \epsilon\right\}\theta\left(2^{1/n}\sigma - r\right)$.[43] The Mie potential is truncated at its minimum, located at $r = 2^{1/n}\sigma$, so that the interaction remains purely repulsive. To approximate the hard-disk limit, we choose a large exponent $n = 32$. The cutoff distance is set to $2^{1/n}\sigma = \sigma_d$ to avoid any discontinuities in the force. The stochastic term $\boldsymbol{\xi}_i^{(j)}$ is a Gaussian white noise with zero mean and covariance determined by the fluctuation–dissipation theorem,

$$\langle \boldsymbol{\xi}_i^{(j)}(t) \rangle = 0, \quad \langle \boldsymbol{\xi}_i^{(j)}(t) \cdot \boldsymbol{\xi}_{i'}^{(j')}(t') \rangle = 2\gamma k_{\mathrm{B}} T \, \delta_{ii'} \delta_{jj'} \, \delta(t - t'), \tag{2}$$

where k_B is the Boltzmann constant and T is the ambient temperature. The self-propulsion force acting on each dumbbell is modeled as $\mathbf{F}_i^{\mathrm{act}} = f_a \frac{\left(\mathbf{r}_i^{(2)} - \mathbf{r}_i^{(1)}\right)}{\left|\mathbf{r}_i^{(2)} - \mathbf{r}_i^{(1)}\right|}$, where f_a denotes the self-propulsion strength, and $\mathbf{r}_i^{(2)} - \mathbf{r}_i^{(1)}$ defines the bond vector connecting the $j = 2$ and $j = 1$ monomers of the ith dumbbell.

The dynamics of a rigid dumbbell can be decomposed into translational motion of its center of mass and rotational motion about the center of mass. The net force and torque acting on the dumbbell are obtained by summing the individual forces and torques acting on its constituent disks. The angular velocity ω_i of the ith rigid dumbbell is identical for both $j = 2$ and $j = 1$ disks and is updated according to

$$I\dot{\boldsymbol{\omega}}_i = \sum_{j=1}^{2}\left[(\boldsymbol{r}_i^{(j)} - \boldsymbol{R}_{\rm com}) \times \nabla_i^j U\right] - \frac{\gamma\sigma_d^2}{2}\boldsymbol{\omega}_i + \sqrt{k_B T\gamma\sigma_d^2}\boldsymbol{\eta}_{ri}, \quad (3)$$

where I is the moment of inertia and $\mathbf{R}_{\rm com}$ denotes the position of the center of mass of each dumbbell. The center of mass of the ith dumbbell obeys

$$2m\dot{\boldsymbol{V}}_{\rm com,i} = -2\gamma\boldsymbol{V}_{\rm com,i} + \sum_{j=1}^{2}\nabla_i^{(j)}U + 2\boldsymbol{F}_i^{\rm act} + \sqrt{4k_B T\gamma}\boldsymbol{\eta}_{ti}, \quad (4)$$

where $\boldsymbol{V}_{\rm com,i}$ denotes the velocity of the center of mass of the ith dumbbell. $\boldsymbol{\eta}_{ti}$ and $\boldsymbol{\eta}_{ri}$ are the Gaussian random forces and torques on the center of mass of the ith dumbbell with zero mean and unit variances, respectively. The translational velocity of each disk is then given by $\dot{\boldsymbol{r}}_i^{(j)} = \boldsymbol{V}_{\rm com,i} + \boldsymbol{\omega}_i \times (\boldsymbol{r}_i^{(j)} - \boldsymbol{R}_{\rm com})$. All physical quantities are expressed in reduced units based on the characteristic scales of the system: mass m, length σ_d, and the energy scale ϵ. Accordingly, the unit of time is defined as $\tau = \sqrt{\frac{m\sigma_d^2}{\epsilon}}$. Throughout this work, we set the thermal energy to $k_B T = 0.01\epsilon$. The integration time step is fixed at $dt = 10^{-3}\tau$, which gives good energy conservation, including the active contribution in the steady state across the entire parameter range considered.

The behavior of the system is governed by several key dimensionless parameters. The first is the Péclet number, which quantifies the relative strength of active forces compared to thermal fluctuations and is defined in Eq. (5) as

$$\mathrm{Pe} = \frac{2\sigma_d f_a}{k_B T}. \quad (5)$$

The second dimensionless parameter Γ in Eq. (6) characterizes the importance of inertial effects and is interpreted as the ratio of two timescales: the momentum relaxation time $\tau_m = \frac{m}{\gamma}$ and the time $\tau_a = \frac{\sigma_d}{f_a/\gamma}$ it takes for a particle to travel its own diameter under self-propulsion,

$$\Gamma = \frac{m f_a}{\gamma^2\sigma_d}. \quad (6)$$

The third parameter is the area fraction defined in Eq. (7) as

$$\phi = \frac{N\pi\sigma_d^2}{2L^2}. \quad (7)$$

The simulations are performed using a custom-modified version of the LAMMPS software.[44]

III. RESULTS

When active forces dominate over thermal fluctuations, rigid dumbbells with orientations that, on average, point toward a common center exert opposing forces on each other (Fig. 1). This leads to the formation of persistent clusters, which continuously grow through coarsening, ultimately resulting in a phase-separated state for overdamped systems. In this work, we investigate the translational and rotational kinetic temperatures of the dumbbell system within the phase-separated regime, defined respectively as $\frac{1}{2}M_{\rm com}\langle V_{\rm com}^2\rangle$ and $\frac{1}{2}I\langle\omega_{\rm com}^2\rangle$. Following the law of energy equipartition, we define the translational and rotational kinetic temperatures in Eqs. (8) and (9), respectively, as

$$T_{\rm trans} = \frac{1}{2}M_{\rm com}\langle V_{\rm com}^2\rangle/k_B, \quad (8)$$

$$T_{\rm rot} = I\langle\omega_{\rm com}^2\rangle/k_B. \quad (9)$$

To ensure overdamped dynamics, we set the friction coefficient to $\gamma = 10$, such that the characteristic time scales associated with translational and rotational inertia remain much smaller than the persistence time of an individual dumbbell, $\tau_p = \frac{\gamma\sigma_d^2}{2k_B T}$. For Pe = 100, $\Gamma = 0.01$, $I/m\sigma_d^2 = 0.5$, and $\phi = 0.4$, the active dumbbell system undergoes a phase separation reminiscent of gas–liquid coexistence, and we find that the translational and rotational kinetic temperatures of the dumbbells remain practically identical in both coexisting phases [Figs. 2(a) and 2(b)]. Next, we decrease γ to increase Γ, making the dynamics of the dumbbells underdamped. The homogeneous state remains metastable for a finite time, after which isolated dense clusters nucleate and grow. Only clusters exceeding a critical size survive, eventually leading to macroscopic phase separation. It is noteworthy that high translational inertia typically favors the homogeneous phase when active particles interact via soft repulsive potentials,[22] as active particles tend to pass through one another with effectively no collisions, suppressing clustering. In contrast, in our system, the interaction between active dumbbells is more hard-sphere-like, which facilitates blocking of the active dumbbells and promotes MIPS even at high translational inertia. In previous studies,[22] the translational kinetic energy of active disks in the dense phase was found to be lower than in the dilute phase. A similar trend for $\frac{1}{2}M_{\rm com}\langle V_{\rm com}^2\rangle$ is observed in our simulations of active dumbbells at $Pe = 100$, $\Gamma = 5.06$, $I/m\sigma_d^2 = 1.0$, and $\phi = 0.4$, where the dense phase appears translationally colder than the dilute phase [Fig. 2(c)]. However, in this case, we do not observe any significant difference in the rotational kinetic energy, $\frac{1}{2}I\langle\omega_{\rm com}^2\rangle$, between the coexisting phases in Fig. 2(d), despite the fact that the interactions responsible for rotational motion are influenced by activity. This indicates that, in anisotropic underdamped active systems, energy dissipation mechanisms for translation and rotation can differ markedly between the coexisting phases of MIPS. However, the interface separating the two phases is not sharp; rather, it is smeared out, with physical quantities varying continuously across a finite interfacial width. This behavior also applies to both translational and rotational temperature profiles. Capillary wave fluctuations significantly contribute to the broadening of the interface.[45]

Next, we construct the phase diagram by varying the Péclet number, Pe, and the area fraction, ϕ, while keeping the translational and rotational inertia fixed at $\Gamma = 5.06$ and $I/m\sigma_d^2 = 1.0$, respectively (Fig. S1). We distinguish homogeneous and MIPS states via the distribution of the local packing fraction. We sampled the local packing fraction as follows. First, the system is divided into square cells. For each cell, we compute a coarse-grained local density by averaging the particle density within a circular region of radius $20\sigma_d$ centered at the cell. From the resulting set of local values, we constructed the corresponding probability distribution function. The dense and dilute phases are identified by distinct peaks in the resulting bimodal distribution of local packing fractions, as is characteristic of MIPS.

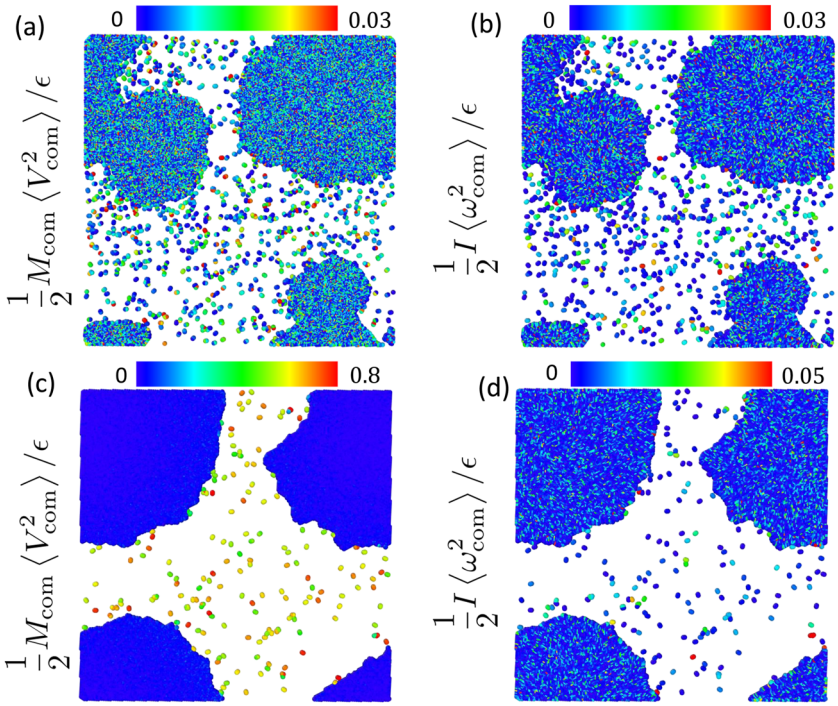

FIG. 2. Panels (a)–(d) show the snapshots from our simulations in the steady state. Panels (a) and (c) are colored according to the translational kinetic energy, $\frac{1}{2}M_{com}\langle V_{com}^2\rangle$, of individual dumbbells, while panels (b) and (d) are colored according to the rotational kinetic energy, $\frac{1}{2}I\langle\omega_{com}^2\rangle$, both expressed in units of ϵ. All simulations are performed at area fraction $\phi = 0.4$ with $N = 16\,129$ dumbbells. The parameters for (a) and (b) are Pe = 100, $\Gamma = 0.01$, and $I/m\sigma_d^2 = 0.5$, and the same for (c) and (d) are Pe = 100, $\Gamma = 5.06$, and $I/m\sigma_d^2 = 1$. For visual clarity, the dumbbell sizes are enlarged and are not shown to scale.

In contrast, the homogeneous phase is characterized by a unimodal distribution.

Our results show that phase separation occurs at sufficiently large area fractions and Péclet numbers. However, inertia suppresses MIPS at low area fractions ($\phi \approx 0.2$–0.3), even at high Pe, in contrast to overdamped dumbbells, which exhibit MIPS under similar conditions.[35] This behavior can be understood as a consequence of inertial effects: upon collision, active inertial dumbbells tend to bounce back directly, thereby increasing their average separation, as observed in the dilute phase of Figs. 2(c) and 2(d). At higher area fractions, this effect is reduced due to the increased frequency of collisions.

To better characterize the structure of the dense phase in the active dumbbell system, we examine the local packing arrangement within the MIPS cluster using a zoomed-in image and its corresponding Delaunay triangulation (Fig. S2). The dense phase is an active crystal[46] that exhibits locally triangular positional order with dislocations similar to those observed for passive granular[47] and colloidal systems.[48,49]

We choose $\gamma = 10\tau^{-1}$ as the reference system, where the dynamics are overdamped and both the translational and rotational kinetic temperatures of the coexisting phases are equal to 0.01, corresponding to the ambient temperature of our simulations as shown in the upward-pointing triangle in Fig. 3(a) and the downward-pointing triangle in Fig. 3(b). To investigate the role of translational inertia, we vary the friction coefficient γ, noting that the Γ scales as γ^2, while keeping the moment of inertia I and active force f_a fixed. A decrease in γ increases the inertial time scale, eventually making it

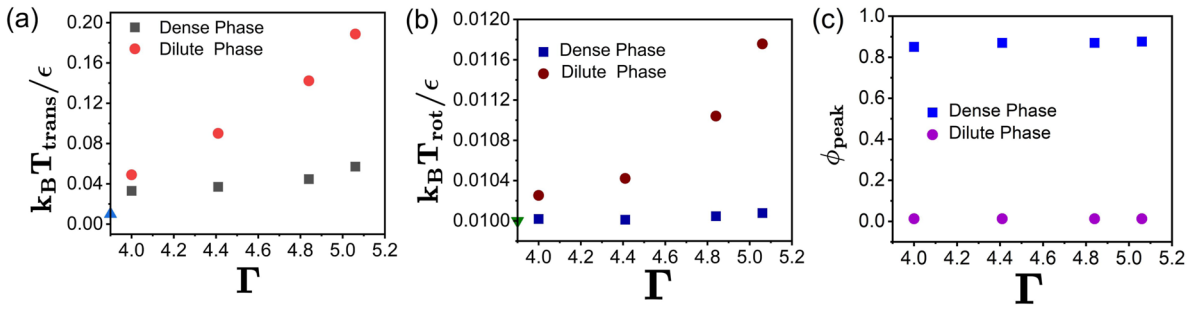

FIG. 3. Panels (a)–(c) show the translational kinetic temperature, rotational kinetic temperature, and the local packing fraction peak value in the coexisting dense and dilute phases of active dumbbells as functions of the dimensionless translational inertia Γ for Pe = 100, $I/m\sigma_d^2 = 0.5$, and $\phi = 0.4$. The ambient temperature, $T = 0.01$, is indicated by the upright triangle on the T_{trans}-axis in (a) and the inverted triangle on the T_{rot}-axis in (b).

comparable to the persistence time scale, τ_p. As a result, the instantaneous particle velocity becomes governed by both the active force and inertia. We observe that the translational kinetic temperature T_{trans} in the dilute phase increases substantially with increasing Γ, whereas the increase is much less pronounced in the dense phase [Fig. 3(a)]. In contrast, the difference in rotational kinetic temperature, T_{rot}, between the coexisting phases also grows with Γ [Fig. 3(b)], but the difference is much smaller than the corresponding difference in T_{trans}. These observations motivate us to analyze the local packing fraction of the system. However, we find that the density difference between the coexisting phases remains nearly unchanged with varying Γ [Fig. 3(c)]. These results demonstrate that an increase in translational inertia exerts a stronger influence on the particles' instantaneous velocities than on their local structural organization. Consequently, the translational kinetic temperature difference between the dense and dilute phases increases monotonically. In the dilute phase, infrequent collisions enable dumbbells to sustain relatively high translational velocities under reduced friction. In contrast, within the dense phase, restricted available space and frequent collisions lead to pronounced dissipation of translational kinetic energy, rendering the dense droplet translationally cold. The response of the rotational degrees of freedom exhibits a distinct behavior. In the dilute phase, rotational motion remains largely unaffected by decreasing friction due to the absence of interparticle interactions. In the dense phase, although activity enhances interactions, rotational motion involves minimal spatial rearrangement. As a result, translational inertia has only a weak influence on the rotational kinetic temperature difference between the two phases.

To gain insight into the role of rotational inertia on kinetic temperature differences, we systematically vary the rotational inertia I while keeping the translational inertia parameters—mass m, bead separation σ_d, active force magnitude f_a, and friction coefficient γ—fixed. As shown in Fig. 4(a), the translational kinetic temperature T_{trans} in the dilute phase increases significantly with increasing rotational inertia $I/m\sigma_d^2$, while the dense phase remains relatively unaffected. This indicates that the translational kinetic temperature difference between the coexisting phases is more strongly influenced by rotational inertia, I, than by translational inertia, Γ. This behavior can be attributed to an increase in the persistence time of active dumbbells with increasing rotational inertia. The active dumbbells exhibit more persistent and directed motion in the dilute phase, enhancing their translational kinetic energy.

In contrast, in the dense phase, the dumbbells undergo frequent collisions that dissipate translational energy, thereby limiting the translational kinetic temperature increase as compared to the dilute phase. Interestingly, the rotational kinetic temperature exhibits a different trend. With increasing rotational inertia I, the rotational kinetic temperature difference in the coexisting phases becomes practically independent of the rotational inertia I [Fig. 4(b)]. While frequent dumbbell collisions generate activity-induced torques that enhance rotational motion, this effect is counteracted by rotational inertia, which suppresses it, resulting in a rotational kinetic temperature that is independent of I. Similar to [Fig. 3(c)], the density difference between the coexisting phases remains nearly constant with I [Fig. 4(c)]. Thus, the active force contributes to rotational motion predominantly through interparticle interactions, emphasizing the crucial role of collisions in transferring activity to rotational degrees of freedom.

Since the observed temperature differences are induced by activity, we now investigate the effect of the self-propulsion speed of the active dumbbells by increasing the Peclet number, Pe, while keeping both the translational and rotational inertia constant. We find that the kinetic temperature difference between the translational and rotational degrees of freedom increases with increasing Pe [Figs. 5(a) and 5(b)]. For translational motion, the rise in kinetic temperature with Pe is more pronounced in the dilute phase compared to the dense phase. This is because, in the dense phase, frequent collisions dissipate the energy input from self-propulsion, thereby limiting the increase in kinetic temperature. In contrast, the rotational temperature in the dense phase remains elevated above the ambient temperature due to activity-induced interactions. However, it is only weakly affected by increasing *Pe*, as rotational motion is significantly hindered by crowding effects from neighboring dumbbells. In the dilute phase, although collisions are infrequent, the increase in self-propulsion speed not only reduces the time between successive collisions but also enhances the magnitude of energy transfer to the rotational degrees of freedom, resulting in a *Pe*-dependent increase in rotational kinetic energy. Overall, the dominant contribution to the kinetic temperature differences in both translational and rotational motion arises from the enhanced mobility in the dilute phase relative to the dense phase.

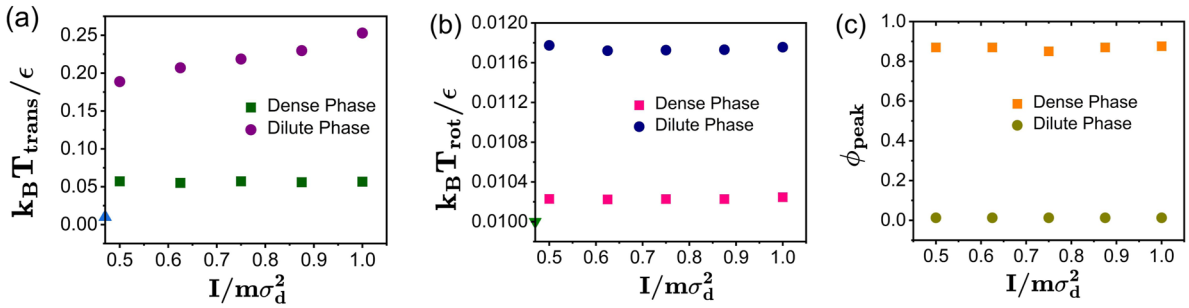

FIG. 4. Panels (a)–(c) show the translational kinetic temperature, rotational kinetic temperature, and the local packing fraction peak value in the coexisting dense and dilute phases of active dumbbells as functions of the dimensionless rotational inertia $I/m\sigma_d^2$ for Pe = 100, Γ = 5.06, and ϕ = 0.4. The ambient temperature, T = 0.01, is indicated by the upright triangle on the T_{trans}-axis in (a) and the inverted triangle on the T_{rot}-axis in (b).

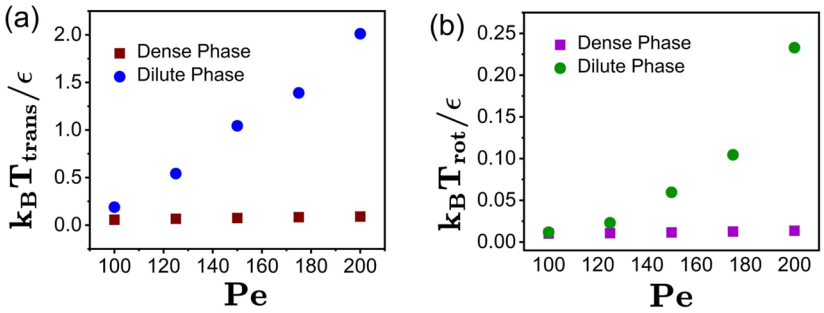

FIG. 5. Panels (a) and (b) show the translational kinetic temperature and rotational kinetic temperature in the coexisting dense and dilute phases of active dumbbells as functions of the dimensionless Peclet number Pe for $\Gamma = 5.06$, $I/m\sigma_d^2 = 0.5$, and $\phi = 0.4$.

IV. CONCLUSION

In this work, we have investigated the dynamics of inertial active dumbbell systems in the regime of motility-induced phase separation (MIPS), focusing on the kinetic temperature differences between the coexisting dense and dilute phases. As a result, the equipartition of translational and rotational temperature, which is valid in equilibrium, is strongly broken by activity. In the phase-separated state, there are four different kinetic temperatures, which all differ from each other, namely, a translational temperature in the dilute and dense phases and a rotational temperature in the dense and dilute phases.

In particular, we have studied here the role of rotational inertia, independent of translational inertia, to probe the effect of activity-induced interactions on kinetic temperature imbalances of the coexisting phases. We find that the system maintains persistent translational and rotational kinetic temperature differences between the coexisting phases during MIPS. Notably, both components of kinetic temperature in the dense and dilute phases exceed the ambient temperature and increase strongly with the self-propulsion speed. This confirms a continuous energy input from the active forces and the absence of thermal equilibrium. Our results reveal that the translational kinetic temperature difference is more sensitive to changes in translational inertia than its rotational counterpart, since the rotational motion is more strongly influenced by inter-particle collisions than the translational motion. Conversely, increasing rotational inertia significantly impacts the translational kinetic temperature difference by enhancing the persistence of active motion. However, the rotational kinetic temperature difference remains unaffected with increasing the rotational inertia to maintain the distinct energy-equipartition for rotational degrees of freedom in coexisting phases. These findings highlight the complex kinetic temperature behavior in anisotropic active systems and underscore the importance of particle shape and rotational degrees of freedom in nonequilibrium phase behavior.

Our results provide concrete predictions for experimental systems, such as vibrated granular particles, where both translational and rotational inertia can be systematically tuned.[50–56] For future studies, it would be interesting to investigate the role of inertia in inhomogeneous but non-phase-separated systems, such as sedimenting active suspensions where gradients are externally imposed.[57,58] A possible experimental setup to observe these effects is active vibrobots on a tilted plane.[59] In our model, the density difference between phases governs the kinetic temperature difference. This suggests that similar temperature differences may also arise in sedimenting active colloids, even in the absence of phase separation. Another promising direction is to generalize the framework developed in this work to spherical particles interacting via anisotropic pair potentials. In this context, a novel type of nonequilibrium phase separation—referred to as flocking phase separation—has been observed in systems of inertial magnetic spheres with dipolar interactions.[60] Extending our framework to incorporate such effects could provide valuable insights for inertial MIPS in anisotropic active matter more broadly.

SUPPLEMENTARY MATERIAL

The supplementary material includes two figures: Fig. S1 presents the phase diagram, and Fig. S2 shows a representative snapshot of MIPS in the inertial active dumbbell system.

ACKNOWLEDGMENTS

S.C. acknowledges the support from the Alexander von Humboldt Foundation. H.L. acknowledges the support from the Deutsche Forschungsgemeinschaft (DFG) through SPP 2265 under Grant No. LO 418/25.

AUTHOR DECLARATIONS

Conflict of Interest

The authors have no conflicts to disclose.

Author Contributions

Subhasish Chaki: Conceptualization (equal); Data curation (equal); Formal analysis (equal); Funding acquisition (equal); Investigation (equal); Methodology (equal); Project administration (equal); Resources (equal); Software (equal); Supervision (equal); Validation (equal); Visualization (equal); Writing – original draft (equal); Writing – review & editing (equal). **Hartmut Löwen**: Conceptualization (equal); Data curation (equal); Formal analysis (equal); Funding acquisition (equal); Investigation (equal); Methodology (equal); Project administration (equal); Resources (equal); Software (equal); Supervision (equal); Validation (equal); Visualization (equal); Writing – original draft (equal); Writing – review & editing (equal).

DATA AVAILABILITY

The data that support the findings of this study are available from the corresponding author upon reasonable request.

REFERENCES

[1] M. C. Marchetti, J. F. Joanny, S. Ramaswamy, T. B. Liverpool, J. Prost, M. Rao, and R. A. Simha, Rev. Mod. Phys. **85**, 1143–1189 (2013).
[2] J. Elgeti, R. G. Winkler, and G. Gompper, Rep. Prog. Phys. **78**, 56601 (2015).
[3] C. Bechinger, R. Di Leonardo, H. Löwen, C. Reichhardt, G. Volpe, and G. Volpe, Rev. Mod. Phys. **88**, 045006 (2016).
[4] M. R. Shaebani, A. Wysocki, R. G. Winkler, G. Gompper, and H. Rieger, Nat. Rev. Phys. **2**, 181–199 (2020).
[5] M. J. Bowick, N. Fakhri, M. C. Marchetti, and S. Ramaswamy, Phys. Rev. X **12**, 010501 (2022).
[6] M. te Vrugt, B. Liebchen, and M. E. Cates, arXiv: 2507.21621 (2025).
[7] A. Godec and R. Metzler, Phys. Rev. E **92**, 010701 (2015).
[8] I. Buttinoni, J. Bialké, F. Kümmel, H. Löwen, C. Bechinger, and T. Speck, Phys. Rev. Lett. **110**, 238301 (2013).
[9] H. D. Vuijk, S. Klempahn, H. Merlitz, J.-U. Sommer, and A. Sharma, Phys. Rev. E **106**, 014617 (2022).
[10] H. Xu, M. R. Nejad, J. M. Yeomans, and Y. Wu, Proc. Natl. Acad. Sci. U. S. A. **120**, e2219708120 (2023).
[11] I. S. Aranson, Rep. Prog. Phys. **85**, 076601 (2022).
[12] S. Henkes, K. Kostanjevec, J. M. Collinson, R. Sknepnek, and E. Bertin, Nat. Commun. **11**, 1405 (2020).
[13] S. Thapa, N. Lukat, C. Selhuber-Unkel, A. G. Cherstvy, and R. Metzler, J. Chem. Phys. **150**, 144901 (2019).
[14] A. Attanasi, A. Cavagna, L. Del Castello, I. Giardina, T. S. Grigera, A. Jelić, S. Melillo, L. Parisi, O. Pohl, E. Shen, and M. Viale, Nat. Phys. **10**, 691–696 (2014).
[15] G. S. Redner, M. F. Hagan, and A. Baskaran, Phys. Rev. Lett. **110**, 055701 (2013).
[16] Y. Fily and M. C. Marchetti, Phys. Rev. Lett. **108**, 235702 (2012).
[17] J. Palacci, S. Sacanna, A. P. Steinberg, D. J. Pine, and P. M. Chaikin, Science **339**, 936–940 (2013).
[18] M. E. Cates and J. Tailleur, Annu. Rev. Condens. Matter Phys. **6**, 219–244 (2015).
[19] B. Adorjáni, A. Libál, C. Reichhardt, and C. J. O. Reichhardt, Phys. Rev. E **109**, 024607 (2024).
[20] D. McDermott, C. Reichhardt, and C. J. O. Reichhardt, Phys. Rev. E **108**, 064613 (2023).
[21] H. Löwen, J. Chem. Phys. **152**, 040901 (2020).
[22] S. Mandal, B. Liebchen, and H. Löwen, Phys. Rev. Lett. **123**, 228001 (2019).
[23] L. Hecht, S. Mandal, H. Löwen, and B. Liebchen, Phys. Rev. Lett. **129**, 178001 (2022).
[24] J. Feng and A. K. Omar, Phys. Rev. E **111**, L043402 (2025).
[25] L. Caprini, R. K. Gupta, and H. Löwen, Phys. Chem. Chem. Phys. **24**, 24910–24916 (2022).
[26] S. De Karmakar and R. Ganesh, Soft Matter **18**, 7301–7308 (2022).
[27] L. Hecht, I. Dong, and B. Liebchen, Nat. Commun. **15**, 3206 (2024).
[28] L. Hecht, L. Caprini, H. Löwen, and B. Liebchen, J. Chem. Phys. **161**, 224904 (2024).
[29] T. S. Ursell, J. Nguyen, R. D. Monds, A. Colavin, G. Billings, N. Ouzounov, Z. Gitai, J. W. Shaevitz, and K. C. Huang, Proc. Nat. Acad. Sci. U. S. A. **111**, E1025–E1034 (2014).
[30] W. F. Paxton, K. C. Kistler, C. C. Olmeda, A. Sen, S. K. St Angelo, Y. Cao, T. E. Mallouk, P. E. Lammert, and V. H. Crespi, J. Am. Chem. Soc. **126**, 13424–13431 (2004).
[31] A. Kudrolli, G. Lumay, D. Volfson, and L. S. Tsimring, Phys. Rev. Lett. **100**, 058001 (2008).
[32] Ö. Duman, R. E. Isele-Holder, J. Elgeti, and G. Gompper, Soft Matter **14**, 4483–4494 (2018).
[33] M. Abkenar, K. Marx, T. Auth, and G. Gompper, Phys. Rev. E **88**, 062314 (2013).
[34] L. F. Cugliandolo, P. Digregorio, G. Gonnella, and A. Suma, Phys. Rev. Lett. **119**, 268002 (2017).
[35] A. Suma, G. Gonnella, D. Marenduzzo, and E. Orlandini, Europhys. Lett. **108**, 56004 (2014).
[36] I. Petrelli, P. Digregorio, L. F. Cugliandolo, G. Gonnella, and A. Suma, Eur. Phys. J. E **41**, 128 (2018).
[37] K. Harth, T. Trittel, S. Wegner, and R. Stannarius, Phys. Rev. Lett. **120**, 214301 (2018).
[38] T. Trittel, K. Harth, and R. Stannarius, Phys. Rev. E **95**, 062904 (2017).
[39] A. R. Sprenger, L. Caprini, H. Löwen, and R. Wittmann, J. Phys.: Condens. Matter. **35**, 305101 (2023).
[40] B. Valecha, H. Vahid, P. L. Muzzeddu, J.-U. Sommer, and A. Sharma, Soft Matter **21**, 3384–3392 (2025).
[41] E. Schiltz-Rouse, H. Row, and S. A. Mallory, Phys. Rev. E **108**, 064601 (2023).
[42] A. Akintunde, P. Bayati, H. Row, and S. A. Mallory, J. Chem. Phys. **162**, 164902 (2025).
[43] G. Mie, Ann. Phys. **316**, 657–697 (1903).
[44] A. P. Thompson, H. M. Aktulga, R. Berger, D. S. Bolintineanu, W. M. Brown, P. S. Crozier, P. J. In't Veld, A. Kohlmeyer, S. G. Moore, T. D. Nguyen *et al.*, Comput. Phys. Commun. **271**, 108171 (2022).
[45] J. Bialké, J. T. Siebert, H. Löwen, and T. Speck, Phys. Rev. Lett. **115**, 098301 (2015).
[46] A. M. Menzel, T. Ohta, and H. Löwen, Phys. Rev. E **89**, 022301 (2014).
[47] C. J. Olson, C. Reichhardt, M. McCloskey, and R. J. Zieve, Europhys. Lett. **57**, 904–910 (2002).
[48] S. J. Gerbode, U. Agarwal, D. C. Ong, C. M. Liddell, F. Escobedo, and I. Cohen, Phys. Rev. Lett. **105**, 078301 (2010).
[49] S. J. Gerbode, S. H. Lee, C. M. Liddell, and I. Cohen, Phys. Rev. Lett. **101**, 058302 (2008).
[50] D. Volfson, A. Kudrolli, and L. S. Tsimring, Phys. Rev. E **70**, 051312 (2004).
[51] M. Gonzalez-Pinto, F. Borondo, Y. Martínez-Ratón, and E. Velasco, Soft Matter **13**, 2571–2582 (2017).
[52] V. Yadav *et al.*, Phys. Rev. E **88**, 052203 (2013).
[53] V. Narayan, S. Ramaswamy, and N. Menon, Science **317**, 105–108 (2007).
[54] C. Scholz, S. Jahanshahi, A. Ldov, and H. Löwen, Nat. Commun. **9**, 5156 (2018).
[55] L. Caprini, A. Ldov, R. K. Gupta, H. Ellenberg, R. Wittmann, H. Löwen, and C. Scholz, Commun. Phys. **7**, 52 (2024).
[56] J. Deseigne, O. Dauchot, and H. Chaté, Phys. Rev. Lett. **105**, 098001 (2010).
[57] V. Carrasco-Fadanelli and I. Buttinoni, Phys. Rev. Res. **5**, L012018 (2023).
[58] J. Palacci, C. Cottin-Bizonne, C. Ybert, and L. Bocquet, Phys. Rev. Lett. **105**, 088304 (2010).
[59] L. Caprini, D. Breoni, A. Ldov, C. Scholz, and H. Löwen, Commun. Phys. **7**, 343 (2024).
[60] N. Luo, L. Li, M. Yang, and Y. Peng, Phys. Rev. Lett. **135**, 178301 (2025).